Macromolecules

NOTE

pubs.acs.org/Macromolecules

Competition between Conformational and Chemical Equilibrium in Suspensions of Polyelectrolyte-Coated Particles

Carl Bartels[†] and David Ronis[*,‡]

[†]Department of Chemistry, University of Manitoba, Winnipeg, Manitoba, Canada R3T 2N2

[‡]Department of Chemistry, McGill University, 801 Sherbrooke West, Montreal, Quebec, Canada H3A 2K6

INTRODUCTION

The stability, phase, optical, and rheological properties of suspensions of nanoparticles and colloidal particles are often intimately connected to the surfactants or surface grafted chains attached to the particles' surfaces. These systems have been of great interest since the 1990s due to their potential applications in many disciplines, most importantly as drug delivery platforms in pharmacology[1] as well as in self-assembly[2−4] and nanoparticle optical properties.[4] The applications often rely on the wide range of morphologies that are available to block copolymers when manipulated under appropriate conditions.[2,5] In all these examples, the chemistry and conformation of the corona or polymer coating layer play a key role in moderating and stabilizing the observed behavior.

In contrast to the wealth of experimental data on these systems (in particular, see refs 5−7), the theoretical understanding of what happens in the corona of these systems when in solution is still quite crude, often restricted to planar surfaces, scaling arguments, infinite dilution, or rigid polyelectrolyte conformations,[8−14] and in particular does not include the effects of chemical equilibrium (something that is only justifiable for strong acid or base monomers and/or at high enough levels of screening where electrostatic interactions between the ionizable monomers can be neglected). Notable exceptions are the works of Leermakers et al.[15] on brushes on flat surfaces using a phenomenological free energy approach and the related work of Klein Wolterink et al.[16] and of Nap et al.[17] on spherical (or planar or cylindrical) systems. As far as we know, none have included chemical equilibrium and interaggregate correlations self-consistently, although Linse's[18] full Monte Carlo simulations of short-chain diblock polyampholyte coronas (with permanent degrees of ionization per monomer) do calculate correlation functions.

As just mentioned, the works of refs 16 and 17 are based on self-consistent free energy calculations which, while capturing many of the intra-aggregate features, ignore any detailed effects of correlations between particles, something that is justified only at high aggregate dilution. Nonetheless, as we will see, many of our results are in qualitative agreement with their calculations. In addition, their work on so-called strong acid or base coronas agrees with our earlier work on these systems, specifically, with respect to strong chain stretching under poor screening conditions, resulting in crystalline-like or defected, rigid-rod-like conformations as discussed in refs 19−21. In addition, density profiles, form factors, interaggregate correlations, the effects of screening, etc., were presented in these works.

Here we extend our approach to include chemical equilibrium by using combinations of liquid-state integral equations and mean-field Monte Carlo simulations[19−24] to explicitly determine variations in the linear backbone charge density of the brush. These variations are the result of the ionization equilibrium in the corona and must be determined in a way that is self-consistent with other aspects of the model, i.e., with intra- and interparticle conformations and correlations. The results presented here highlight some of the more dramatic effects that can be seen in the corona of block copolymer micelles with a polyelectrolyte corona when dissolved in water under different conditions of pH and ionic strength. In particular, under conditions that lead to intermediate levels of ionization, the free energy difference between stretched, more ionized, chains and random, more neutral, ones can be very slight, resulting in a conformational frustration in the chains in the corona of a micelle, leading to bimodal monomer distributions in qualitative agreement with the results of refs 16 and 17.

The *ad hoc* assumption of uniform charge density along the chains of the corona precludes any cooperative ionization phenomena; specifically, ionization in one region of the chain decreasing the likelihood the nearby portions of the chain will also become ionized. The interplay between the free energy of ionization, the free energy changes associated with conformational changes, screening, and Coulombic interactions within the brush can lead to new phases within the corona. Like Klein Wolterink et al.,[16] not only do we account for these phenomena by allowing the self-consistent variation of ionization along the brush, but in addition our approach still predicts colloid−colloid and colloid−counterion correlations that can be tested experimentally. This can be contrasted to previous versions of this model which did not properly account for the variations of charge density or even alternative models such as the DPD[25] or even older blob[26] models which make weaker predictions.

THEORY

Interparticle Potentials and Correlations. The work presented here extends earlier models for charged colloids[22] and those coated by a neutral or polyelectrolyte brush,[19−21,23] and the reader is referred to these references for a discussion of the integral-equation formalism and approximations. In short, the

Received: October 13, 2010
Revised: March 4, 2011
Published: March 17, 2011

overall approach is based on the Ornstein−Zernike (OZ) equations for systems consisting of several species. Each species, i, has its own charge, q_i, and its own bulk concentration, ρ_i. In this case, the total correlation functions, $h_{i,j}$, and direct correlation functions, $c_{i,j}$, for each pair of species are related to one another through the OZ equations (as Fourier transforms)

$$\tilde{h}_{i,j}(k) = \tilde{c}_{i,j}(k) + \sum_l \tilde{c}_{i,l}(k)\rho_l\tilde{h}_{l,j}(k) \quad (1)$$

where the subscripts denote different species, ρ_l is the bulk concentration of species l, and, henceforth, the tilde denotes a spatial Fourier transform. We treat the solvent as a continuum with dielectric constant ε. As was shown in ref 20, as long as the small ions are considered as points in the mean spherical approximation, the problem can be transformed into one with a single effective counterion, with effective charge and concentration z_p and ρ_p, respectively, and neutral point particles. In this way, eq 1 is reduced to an OZ equation for a two-component system, with the main problem being a matter of determining the colloid−colloid and colloid−effective ion distributions. The "c" and "p" subscripts will be used to denote the colloid and effective counterion species.

In order to solve the set of coupled equations represented by eq 1, we need a set of closure conditions. In the case of the colloid−effective counterion correlations, the mean spherical approximation (MSA) is used, i.e.

$$h_{p,c}(r) = -1 \quad (r \le R_{p,c}) \quad (2)$$

and

$$c_{p,c}(r) = -\beta u_{p,c}(r) \quad (r > R_{p,c}) \quad (3)$$

where $R_{p,c}$ is the closest approach distance of the effective counterion and colloid centers of mass, $\beta = 1/k_bT$, k_b is Boltzmann's constant, and T is the absolute temperature; $u_{p,c}$ is the potential for the interaction between the colloid and a single effective counterion and will be discussed later. Since the counterions have been assumed to be points, the MSA simply states that $c_{p,p}(r) = -\beta u_{p,p}(r) = -\beta z_p^2/\varepsilon r$.

As was shown in ref 20, the p−c correlations can be explicitly determined in terms of the c−c ones for *arbitrary* $u_{p,c}(r)$ within the corona. The distribution of counterions around a colloid modifies the interaction potential between colloid particles; what remains is a one-component problem with an effective interaction potential that can be used in closures such as the hypernetted-chain approximation (HNC), i.e.

$$\beta\tilde{u}_{c,c;\mathrm{eff}}(k) = \beta\tilde{u}_{c,c}(k) - \frac{\rho_p k^2 \tilde{c}_{p,c}^2(k)}{k^2 + \kappa^2} \quad (4)$$

where $\tilde{u}_{c,c}(k)$ is the Fourier transform of the unmodified potential and κ is the Debye screening wave vector $(1/\lambda_D)$ and where the reader is referred to ref 20 for the detailed form of $c_{p,c}(r)$. The HNC closure thus becomes

$$g_{c,c}(r) = e^{-\beta u_{c,c;\mathrm{eff}}(r) + h_{c,c}(r) - c_{c,c}(r)} \quad (5)$$

Contributions from the Corona. The preceding results allow us to calculate the local distribution of macroions and more importantly the local counterion densities for arbitrary interaction potentials, $u_{p,c}$ and $u_{c,c}$ (or $u_{c,c;\mathrm{eff}}$). Both depend on the distribution and composition of monomers in the corona and can be written as

$$u_{c,c}(\mathbf{R}) = \sum_{\alpha,\gamma}\int d\mathbf{r}\, d\mathbf{r}'\, \rho_{m,\alpha}(\mathbf{r})u_{\alpha,\gamma}(|\mathbf{r}' + \mathbf{R} - \mathbf{r}|)\rho_{m,\gamma}(\mathbf{r}') \quad (6)$$

and

$$u_{p,c}(\mathbf{r}) = \sum_{\alpha}\int d\mathbf{r}'\, u_{p,\alpha}(|\mathbf{r}' - \mathbf{r}|)\rho_{m,\alpha}(\mathbf{r}') \quad (7)$$

where $\rho_{m,\alpha}(\mathbf{r})$ is the distribution of monomers of type α around the core of a micelle, $u_{\alpha,\gamma}(r)$ is the potential acting between monomers of types α and γ, and $u_{p,\alpha}(r)$ is the potential between a monomer of type α and an effective point ion.

For what follows, a mean-field approximation will be used; i.e., the average $\rho_{m,\alpha}(r)$'s will be used to calculate the various correlation functions. Of course, the local monomer density is very sensitive to the counterion distribution, and vice versa, and hence must be calculated self-consistently. As in the earlier works, this will be accomplished by considering a single chain, or ensemble of independent chains, and sampling conformations by Monte Carlo simulation, from which the $\rho_{m,\alpha}(r)$ can easily be constructed and then used to recalculate the correlations, and so on.

Unlike our earlier works, we do not assume a constant degree of ionization along the chain; rather, local chemical equilibrium will be introduced. We let

$$\rho_{m,\alpha}(r) = f_\alpha(r)\rho_m(r) \quad (8)$$

where $f_\alpha(r)$ and $\rho_m(r)$ are the fraction of monomers in state α and total monomer density at r, respectively. By viewing the ionization equilibrium as an ideal binding equilibrium,[15−17,24,27] it follows that

$$f_\alpha(r) = \frac{e^{-\beta(\phi_\alpha(r) - \mu_\alpha)}}{\sum_\gamma e^{-\beta(\phi_\gamma(r) - \mu_\gamma)}} \quad (9)$$

where $\phi_\alpha(r)$ is the average energy of a monomer of type α at r and μ_α is its bulk chemical potential. The exact $\phi_\alpha(r)$'s are quite complicated, depending on the chain conformations and counterion distributions; here they will be treated within a mean field approximation, i.e.

$$\beta\phi_\alpha(r) = q_\alpha\beta\Phi_E(r) + \sum_\gamma \nu_{\alpha,\gamma}(f_\gamma(r)\rho_m(r) + \int d\mathbf{r}'\, f_\gamma(r')\rho_m(r')\rho_c g_{c,c}(|\mathbf{r} - \mathbf{r}'|)) \quad (10)$$

where the $\nu_{\alpha,\gamma}$'s are Flory excluded volume parameters and $\Phi_E(r)$ is the local electrical potential. The term with the integral represents interaggregate monomer−monomer excluded volume interactions. The local electrical potential is most succinctly expressed as its Fourier transform

$$\tilde{\Phi}_E(k) = \frac{4\pi}{\varepsilon k^2}\left(\sum_\alpha q_\alpha\tilde{\rho}_{m,\alpha}(k)[1 + \rho_c\tilde{h}_{c,c}(k)] + q_p\rho_p\tilde{h}_{p,c}(k)\right) \quad (11)$$

where the terms in $\tilde{h}_{c,c}$ and $\tilde{h}_{p,c}$ correspond to the charge associated with neighboring macroions or the counterions, respectively.

dx.doi.org/10.1021/ma102336x |*Macromolecules* 2011, 44, 3174–3178

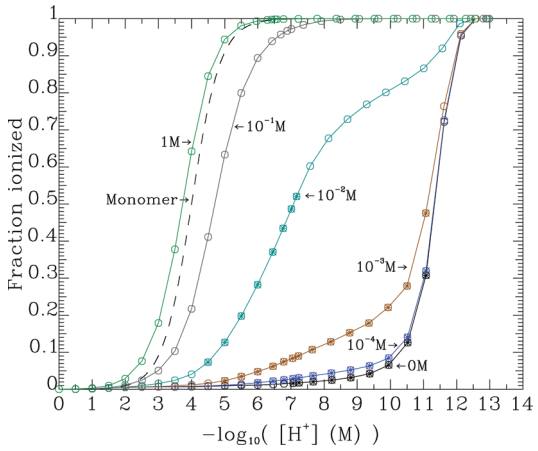

Figure 1. Titration curves at 298 K in water in the presence of added 1:1 electrolyte for infinitely dilute aggregates having 100, 100-monomer-long chains, each monomer has a pK_a of 4.0 (roughly that of acrylic acid), is σ = 2.52 Å long and is grafted to a 50 Å radius core. Here $\nu_{i,j} = 0.22 \times 4\pi\sigma^3/3$. The dashed line is the titration curve for the isolated monomers. Debye−Huckel ionic activities were used. The cases with filled-in points exhibit bimodal end monomer distributions.

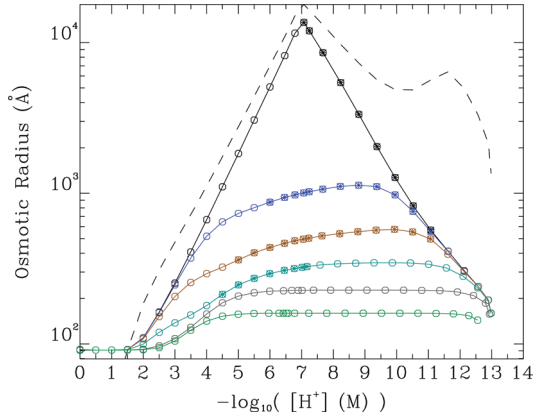

Figure 2. Effective hard-sphere osmotic radii for the cases shown in Figure 1. The poor-screening limiting behavior, using the actual colloid charges, is shown for the no added salt case (dashed line).

Finally, the mean potential, $\Phi(r)$, governing the conformation of the corona chains can easily be expressed in terms of the $\phi_\alpha(r)$'s as

$$e^{-\beta\Phi(r)} = \sum_\alpha e^{-\beta(\phi_\alpha(r) - \mu_\alpha)} \qquad (12)$$

up to an unimportant overall additive constant in $\Phi(r)$.

Thus, to recap, the conformations of one or more independent chains are sampled using Monte Carlo, with eq 12 as the potential. Periodically, the current average monomer density is used to calculate the ionization fractions, eq 9, and these are then used to recompute the potentials, eqs 6 and 7, and correlations as described above.

RESULTS AND DISCUSSION

Allowing the monomers to establish their own ionization equilibrium has dramatic effects. If the μ_α are chosen in such a way that the equilibrium of the free monomer corresponds closely to acrylic acid, like Klein Wolterink,[16] we see a marked suppression of ionization of the micelle, particularly at low ionic strengths. This can be seen in the titration curves shown in Figure 1. Basically, having to overcome the ionized monomer−monomer Coulombic repulsion adds a significant free energy cost and results in suppressed ionization. Adding salt screens the interaction and reduces the effect (as does reducing the aggregation number or making the monomers larger). All this is in qualitative agreement with the results of ref 16. Shifts in the ionization curves due to local potentials are not surprising and have been used to measure the local surface potentials;[28] note however that they are much larger here.

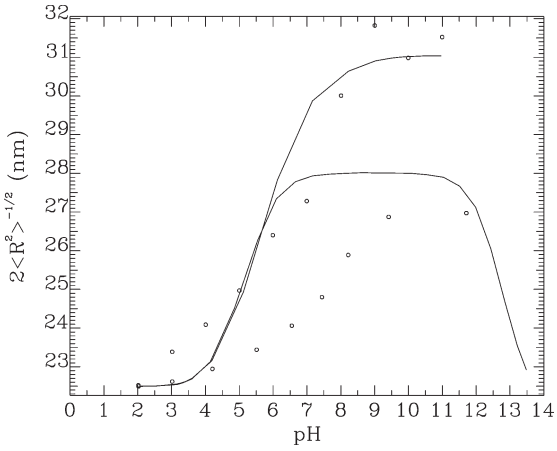

Figure 3. Corona rms diameter for the titration performed by Connal et al.[7] The open circles are the experimental data given in Figure 5 of ref 7. The solid line was calculated for a system comprised of 32 chains, each containing 88 monomers, the first 13 of which (as counted starting from the core) were neutral while the rest had a pK_a of 4.25 (the same as bulk acrylic acid). All monomers were 2.52 Å long and the core had a 5 nm radius. The overall aggregate concentration was 3.8 μM. The $\nu_{i,j}$'s were all set to $62 \times 4\pi\sigma^3/3$, which was fit to the lowest pH experimental result.

Interaggregate repulsions increase as the chains ionize, moderated by screening, and this leads to an increase in the second osmotic virial coefficient. In the McMillan−Mayer theory of solutions $B_2 = 2\pi\int_0^\infty dr\, r^2[1 - g_{c,c}(r)]$. By interpreting this as a hard-sphere osmotic virial coefficient, i.e., $B_2 = 16\pi R^3/3$, where R is an effective osmotic radius, we obtain the results shown in Figure 2. Note that while the degree of ionization increases as the pH is increased, so too does the ionic strength and screening for pH > 7 and results in the turnover seen in the osmotic radii; indeed, when screening is poor, a large portion the osmotic radius simply reflects the length over which the interaggregate electrostatic interactions are screened. In the limit infinite dilution and very poor screening it is easy to show that $B_2 \sim 2\pi z_c^2 \lambda_D^2/(\varepsilon k_B T)$, resulting in the osmotic radii shown in the dashed line in Figure 2. The first maximum occurs when the screening length starts to decrease, while the second appears when the chains ionize, although the poor screening approximation is clearly not valid here. The turnover in osmotic radius will result in strong re-enentrant behavior in poly-ball crystallization phase transitions as was predicted some time ago for surface-charged colloids[22] and seen experimentally.[29] Again, the effects are much larger here. Also note that decreasing the amount of added salt leads to an increase in the osmotic radius; part of this is simply due to the increase in the Debye screening length, but part

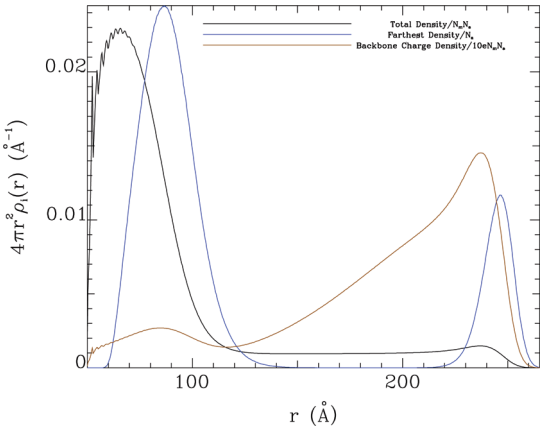

Figure 4. Total monomer, farthest monomer on a single chain, and backbone charge densities for the system depicted in the preceding figures, where now $\rho_c = 2 \times 10^{-7}$ M, in the presence of 10^{-4} M added 1:1 electrolyte and pH = 9.94. Here 10.6% of the monomers are ionized. 50% and 90% of the charge are situated on the outermost 6% and 18% of the monomers, respectively, corresponding to the low-density tail of the monomer distribution.

is due to the strong stretching of the chains.[19−21] This has been observed recently by Jia et al.[30]

Finally, we have compared the rms diameter with the so-called hydrodynamic diameters measured by Connal et al.[7] in Figure 3. In these experiments, a solution, initially at pH 11, was titrated with acid until pH 2 was reached (the upper curve/data) and then with base until the pH was again 11 (the lower curve/data); along the way DLS was performed to measure a radius. According to ref 7, 15% of the chains were not deprotected and hence cannot ionize; we have incorporated this into our calculation by assuming that the undeprotected monomers were near the core and made the first 13 monomers of each chain permanently neutral. Our calculation is a one-parameter fit (the ν's) to the experiment. The overall agreement is reasonable, especially given that the rms diameter is not the hydrodynamic radius measured in DLS and that it is likely that the aggregate corona will shift from a non-free-draining regime to a more free-draining one as the chains stretch. In addition, for the aggregate concentration studied, there are static correlations and interaggregate hydrodynamic interactions that should be taken into account in the stretched (high pH) regime.[31] The calculated results collapse to more or less a single curve at low pH, as expected for a neutral system and point counterions. The role of polyelectrolyte−counterion steric interactions will be examined elsewhere. If we define an effective pK_a as the point where 50% of the monomers are ionized, we get 5.0 and 5.6 for the added acid and added base portions of the experiment, respectively. This is a bit low compared with the value of 6.5 reported in Figure 4 of ref 7 although they are not particularly clear as to what solution conditions were used. Finally, note that we predict that the chains shrink at very high pH, unfortunately just beyond those studied in ref 7, again due to screening of the electrostatic interactions; this downturn may be overestimated as we have assumed point counterions and or Debye−Huckel chemical potentials. In addition, the ionic strength at the high pH end of the base titration is quite large (ca. 1 M), and it is possible that the MSA is breaking down.

The most surprising result of this work is an effect that occurs at intermediate levels of ionization. In the neutral, almost completely un-ionized chain the corona is collapsed and shows behavior similar to what might be expected from an ideal brush. In contrast, the highly ionized chains are driven by Coulomb forces to become almost fully stretched. Both of these behaviors are reasonable and familiar. At intermediate levels of ionization, however, the chains are faced with a choice. One possibility is that all chains behave the same, resulting in similar, intermediate, extents of ionization and stretching. The other possibility is that some chains sacrifice their conformational entropy, becoming highly ionized and extended, while others remain neutral and collapsed. The Monte Carlo results indicate that the latter is the case when the screening is low enough, with a few chains making a large enthalpic gain by extending and ionizing at the expense of entropy.

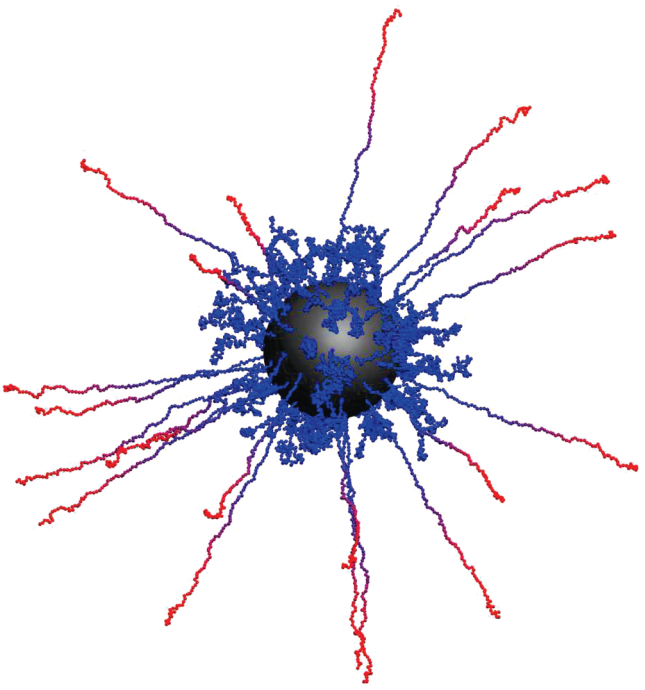

Figure 5. An image generated from one of the configurations of the micelle used to generate the data in Figure 4. The color coding reflects the extent of ionization, with red indicating ionized monomers and blue indicating neutral monomers.

Figure 4 shows the distribution of monomers and chain ends of a typical case. Here most of the charge resides on the outermost monomers. Figure 5 shows a micelle configuration from the same case. Note that there is significant exchange between ionized−stretched and neutral−collapsed chains during the Monte Carlo run that is reminiscent of pseudopods encountered in nature.

Finally, Figure 6 shows some finite concentration, intermacroion results. In particular, note that the counterions are rather loosely held by the chains, extending roughly 4 Debye lengths from the ionized chains; at longer distances the counterion and backbone-ion densities approach each other as required by electroneutrality.

Modifying the existing methods for calculating chain conformations and correlation functions to allow for self-consistent degree of ionization has provided some surprising results. The extent to which ionization is suppressed, even at relatively high ionic strength, is significant. Even more significant is the tendency of the chains in a

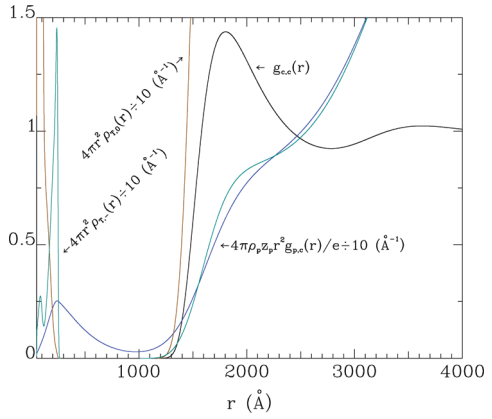

Figure 6. Macroion−macroion pair correlation function, $g_{c,c}(r)$ (black), total (i.e., including contributions from neighboring aggregates) ionized ($\rho_{T,-}(r)$) and neutral ($\rho_{T,0}(r)$) monomer densities (cyan and brown, respectively) and the counterion charge density (blue) for the finite density cases shown in the preceding two figures. The Debye screening length is 177 Å.

micelle to dynamically partition themselves between coiled and extended conformations as a means to balance entropic and enthalpic factors. Our approach treats intra- and interaggregate correlations and interactions on an equal footing (albeit within a mean-field approximation) and results in correlation functions, structure factors, etc. In the future, we will examine some more exotic aggregate systems as well as partially relax the assumption of point counterions.

AUTHOR INFORMATION

Corresponding Author

*E-mail: David.Ronis@McGill.CA.

ACKNOWLEDGMENT

We thank R. Bruce Lennox for useful discussions and the Natural Sciences and Engineering Research Council of Canada for supporting this work.

REFERENCES

(1) See, e.g.: (a) Faraji, A. H.; Wipf, P. *Bioorg. Med. Chem.* **2009**, *17*, 2950. (b) Panyam, J.; Labhasetwar, V. *Adv. Drug Delivery Rev.* **2003**, *55*, 329.

(2) See, e.g.: (a) Kim, H.-C.; Park, S.-M.; Hinsberg, W. D. *Chem. Rev.* **2010**, *110*, 147. (b) Allen, C.; Maysinger, D.; Eisenberg, A. *Colloids Surf., B* **1999**, *16*, 3. (c) Savic, R.; Eisenberg, A.; Maysinger, D. *J. Drug Targeting* **2006**, *14*, 343.

(3) See, e.g.: Claridge, S. A.; Castelman, A. W., Jr.; Khanna, S. N.; Murray, C. B.; Sen, A.; Weiss, P. S. *Nano* **2009**, *3*, 244.

(4) See, e.g.: Talapin, D. V.; Lee, J.-S.; Kovalenko, M. V.; Shevchenko, E. V. *Chem. Rev.* **2010**, *110*, 389.

(5) (a) Zhu, J.; Lennox, R. B.; Eisenberg, A. *J. Am. Chem. Soc.* **1991**, *113*, 5583; (b) *Langmuir* **1991**, *7*, 1579. (c) Zhang, L.; Yu, K.; Eisenberg, A. *Science* **1996**, *272*, 1777. (d) Zhang, L.; Eisenberg, A. *Macromolecules* **1996**, *29*, 8805. (e) Moffitt, M.; Yu, Y.; Nguyen, D.; Graziano, V.; Schneider, D. K.; Eisenberg, A. *Macromolecules* **1998**, *31*, 2190. (f) Lysenko, E. A.; Bronich, T. K.; Eisenberg, A.; Kabanov, V. A.; Kabanov, A. V. *Macromolecules* **1998**, *31*, 4511.

(6) Plamper, F. A.; Becker, H.; Lanzendorfer, M.; Patel, M.; Wittemann, A.; Ballauff, M.; Muller, A. H. E. *Macromol. Chem. Phys.* **2005**, *206*, 1813–1825.

(7) Connal, L. A.; Li, Q.; Quinn, J. F.; Tjipto, E.; Caruso, F.; Qiao, G. G. *Macromolecules* **2008**, *41*, 2620–2626.

(8) Linse, P.; Claesson, P. M. *Macromolecules* **2010**, *43*, 2076.

(9) Leermakers, F. A. M.; Ballauff, M.; Borisov, O. V. *Langmuir* **2008**, *24*, 10026.

(10) Mei, Y.; Hoffmann, M.; Ballauff, M.; Jusufi, A. *Phys. Rev. E* **2008**.

(11) Kumar, N. A.; Seidel, C. *Phys. Rev. E* **2007**, *76*, 020801/1.

(12) Naji, A.; Seidel, C.; Netz, R. R. *Adv. Polym. Sci.* **2006**, *198*, 149.

(13) Harnau, L.; Hansen, J.-P. *J. Chem. Phys.* **2002**, *116*, 9051.

(14) Baratlo, M.; Fazlia, H. *Europhys. J. E* **2009**, *29*, 131.

(15) (a) Lyatskaya, Y. V.; Leermakers, F. A. M.; Fleer, G. J.; Zhulina, E. B.; Birshteint, T. M. *Macromolecules* **1995**, *28*, 3562. (b) Mercurieva, A. A.; Birshtein, T. M.; Zhulina, E. B.; Iakovlev, P.; van Male, J.; Leermakers, F. A. M. *Macromolecules* **2002**, *35*, 4739.

(16) Klein Wolterink, J.; van Male, J.; Cohen Stuart, M. A.; Koopal, L. K.; Zhulina, E. B.; Borisov, O. V. *Macromolecules* **2002**, *35*, 9176–9190.

(17) Nap, R.; Gong, P.; Szleifer, I. *J. Polym. Sci., Part B: Polym. Phys.* **2006**, *44*, 2638.

(18) Linse, P. *J. Chem. Phys.* **2007**, *126*, 114903.

(19) Ronis, D. *Macromolecules* **1993**, *26*, 2016.

(20) Ronis, D. *Phys. Rev. E* **1994**, *49*, 5438.

(21) Ronis, D. *Physica A* **1996**, *231*, 220.

(22) Khan, S.; Morton, T.; Ronis, D. *Phys. Rev. A* **1987**, *35*, 4295.

(23) Ronis, D. *Phys. Rev. A* **1991**, *44*, 3769.

(24) Bartels, C. Coronae of block copolymer micelles as supports for organometallic catalysis. Ph.D. Thesis, McGill University, 2003.

(25) Deng, M.; Jiang, Y.; Li, X.; Wang, L.; Liang, H. *Phys. Chem. Chem. Phys.* **2010**, *12*, 6135.

(26) Biver, C.; Hariharan, R.; Mays, J.; Russel, W. B. *Macromolecules* **1997**, *30*, 1787.

(27) Hill, T. L. *Introduction to Statistical Thermodynamics*; Addison-Wesley Pub. Co.: Reading, MA, 1960; Chapter 5.

(28) Fernadez, M. S.; Fromherz, P. *J. Phys. Chem.* **1977**, *81*, 1755.

(29) Wette, P.; Klassen, I.; Holland-Moritz, D.; Herlach, D. M.; Shope, H. J.; Reiber, N.; Palberg, T.; Roth, S. V. *J. Chem. Phys.* **2010**, *132*, 131102.

(30) Jia, H.; Grillo, I.; Titmuss, S. *Langmuir* **2010**, *26*, 7482.

(31) See, e.g.: Brown, J. C.; Pusey, P. N.; Goodwing, J. W.; Ottewill, R. H. *J. Phys. A: Gen. Phys.* **1975**, *8*, 664.